

# A Fluorinated Sialic Acid Vaccine Lead Against Meningitis B and C

Christina Jordan,<sup>#</sup> Kathrin Siebold,<sup>#</sup> Patricia Priegue,<sup>#</sup> Peter H. Seeberger,<sup>\*</sup> and Ryan Gilmour<sup>\*</sup>



Cite This: *J. Am. Chem. Soc.* 2024, 146, 15366–15375



Read Online

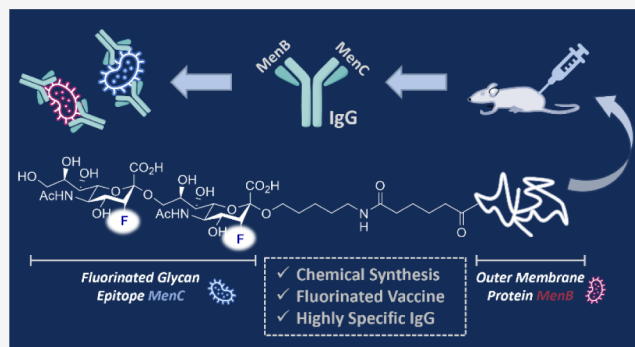
ACCESS |

Metrics & More

Article Recommendations

Supporting Information

**ABSTRACT:** Inspired by the specificity of  $\alpha$ -(2,9)-sialyl epitopes in bacterial capsular polysaccharides (CPS), a doubly fluorinated disaccharide has been validated as a vaccine lead against *Neisseria meningitidis* serogroups C and/or B. Emulating the importance of fluorine in drug discovery, this molecular editing approach serves a multitude of purposes, which range from controlling  $\alpha$ -selective chemical sialylation to mitigating competing elimination. Conjugation of the disialoside with two carrier proteins (CRM197 and PorA) enabled a semisynthetic vaccine to be generated; this was then investigated in six groups of six mice. The individual levels of antibodies formed were compared and classified as highly glycan-specific and protective. All glycoconjugates induced a stable and long-term IgG response and binding to the native CPS epitope was achieved. The generated antibodies were protective against MenC and/or MenB; this was validated *in vitro* by SBA and OPKA assays. By merging the fluorinated glycan epitope of MenC with an outer cell membrane protein of MenB, a bivalent vaccine against both serogroups was created. It is envisaged that validation of this synthetic, fluorinated disialoside bioisostere as a potent antigen will open new therapeutic avenues.



## 1. INTRODUCTION

Societal confidence in vaccination is a key driver of innovation in the design and conception of novel candidates for clinical translation.<sup>1</sup> Of the major classes of biopolymers that take center stage, carbohydrates have proven to be particularly adept.<sup>2</sup> This is a consequence of their structural complexity and diversity.<sup>3</sup> Glycan-based molecular recognition manifests itself across the spectrum of biological function,<sup>4</sup> and is central to the immune response. However, the successful implementation of carbohydrate-based vaccines continues to be frustrated by the low binding affinities of glycan-protein interactions,<sup>5</sup> and the hydrolytic liabilities associated with the glycoside linkages.<sup>6</sup> Medicinal chemistry approaches to enhancing binding affinities and improving the metabolic stability of glycans<sup>7</sup> have been intensively pursued and represent a new frontier in biomedical research.<sup>2e</sup> However, this strategy must be reconciled with the challenges associated with stereocontrolled *de novo* synthesis campaigns and site-selective editing.<sup>8</sup> Inspired by the success of fluorination as a molecular editing strategy in pharmaceutical design,<sup>9</sup> it was reasoned that judicious installation of a C(sp<sup>3</sup>)-F bond proximal to the glycosidic linkage may play a multitude of roles in vaccine development. These include regulating glycosylation,<sup>10</sup> increasing enzymatic stability<sup>7</sup> and providing a valuable NMR active nucleus to facilitate structural determination.<sup>11</sup> Collectively, these attributes provide a compelling argument for the strategic use of fluorinated sugars in vaccine development. Motivated by our observation that the

selective introduction of fluorine at C3 of protected sialic acid donors enables highly  $\alpha$ -selective chemical sialylation,<sup>12</sup> we embarked upon a campaign to validate the advantages of fluorinated sialic acids in vaccine development. This led us to consider the conspicuous  $\alpha$ -(2,9)-sialyl linkage of the *Neisseria meningitidis* serogroup C epitope (1, Figure 1).

The  $\alpha$ -(2,8)-Neu5Ac regioisomer present in the CPS of *N. meningitidis* serogroup B is prevalent in human neuronal glycans and therefore unsuitable as a carbohydrate-based vaccine lead.<sup>13</sup> However, the  $\alpha$ -(2,9)-sialyl epitope is specific for bacterial capsular polysaccharides (CPS), rendering it an appealing synthetic target.<sup>14</sup> The development of a robust, stereocontrolled route would also eliminate concerns regarding contamination of polymeric material directly isolated from the bacterial capsule,<sup>15</sup> and facilitate scale-up.

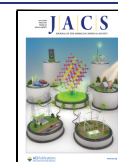
To that end, a chemical sialylation route to the target, fluorinated disialoside 2 (DisAF), was envisaged to allow for the stereoselectivity and reactivity to be attenuated, and suppress competing 2,3-elimination.<sup>16</sup> Reducing the polysaccharide structural motif to a disialoside and adding an amino linker provides a handle for conjugation to a carrier

Received: March 4, 2024

Revised: April 22, 2024

Accepted: April 23, 2024

Published: May 20, 2024



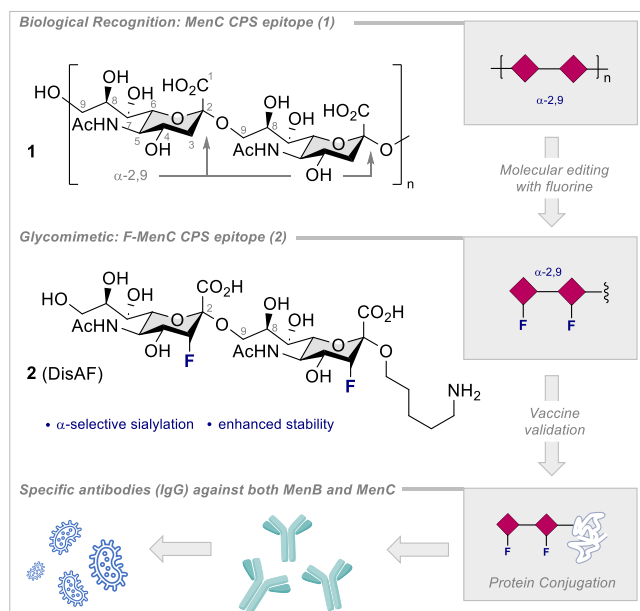


**Figure 1.** Leveraging fluorine-directed sialylation to create a novel glycomimetic for validation in MenB and MenC vaccine development.

protein. Two different carrier proteins and two adjuvants were used to decipher the effect of the immunogenicity. As the CPS of *N. meningitidis* serogroup B cannot be used as a blueprint for a synthetic vaccine, the use of a specific carrier protein (PorA) was envisaged. PorA is part of the commercial vaccine against MenB, but to the best of our knowledge, it has never been used as a carrier protein in this context. By merging the properties of the carbohydrate epitope and carrier protein in the design, it was envisaged that a novel C-3 fluorinated glycoconjugate against both serogroups B and C could be validated. A bivalent vaccine is particularly advantageous in regions where serogroups B and C are most prevalent (Europe, the Americas, Africa, and Australia).

## 2. RESULTS AND DISCUSSION

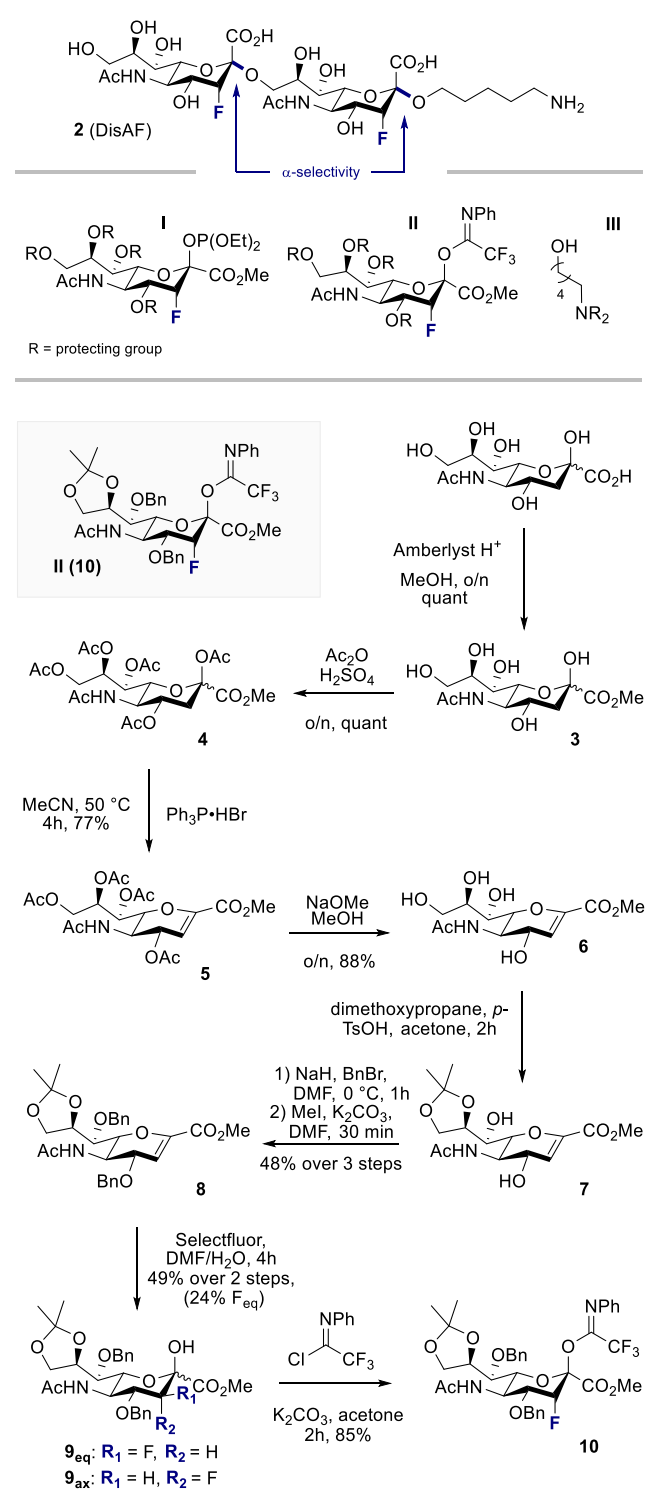
### 2.1. Chemical Synthesis of the Fluorinated Disialoside.

The retrosynthetic analysis of target disaccharide **2** was contingent on the success of two  $\alpha$ -selective sialylation processes that would leverage the directing group effect of the axial C(sp<sup>3</sup>)-F bond. Consequently, the generic building blocks **I**, **II**, and **III** were conceived as bearing appropriate protective group patterns.

Central building block **10** was prepared by the esterification of commercially available *N*-acetylneuraminic acid in the presence of Amberlyst and methanol (Scheme 1, compound **3**) before the acetate protection of the remaining hydroxyl groups produced **4** in quantitative yield over two steps. Elimination using PPh<sub>3</sub>·HBr at 50 °C proved to be operationally simple and forged product **5** with a 77% yield. Importantly, performing these first four steps on a gram scale did not compromise efficiency.

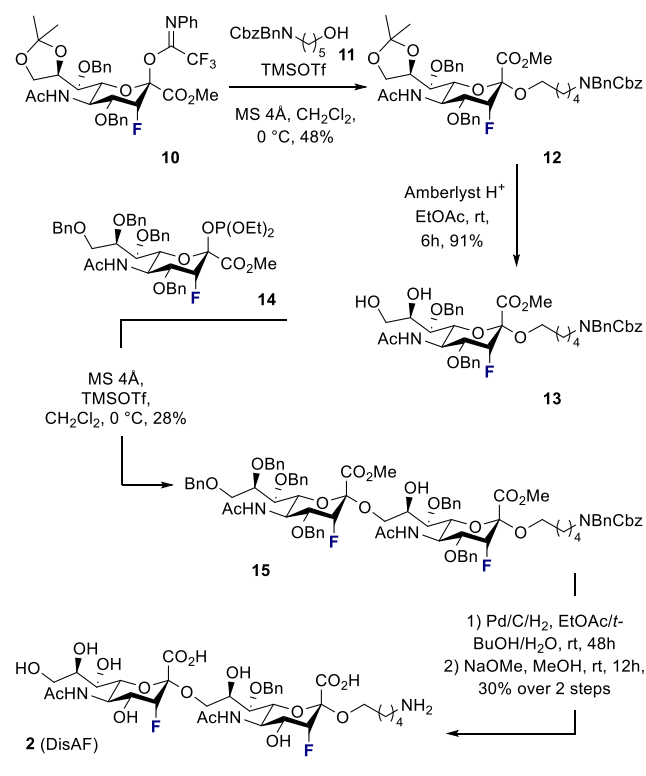
Following acetate hydrolysis to furnish **6**, orthogonal protecting groups were introduced, beginning with the acetonide at the C8/C9 diol (**7**). Subsequent benzylation at the C4 and C7 positions furnished the fluorination precursor **8**. This was smoothly converted to **9** by treatment with Selectfluor.<sup>17</sup> It is important to note that partial cleavage of the acetonide was observed during the fluorination reaction.

### Scheme 1. Retrosynthetic Analysis of Target **2** and Synthesis of Fluorinated Building Block **10**



However, regeneration was facile by treating the crude mixture following work up with *p*-TsOH and dimethoxy propane. Gratifyingly, the ratio of equatorial (**9**<sub>eq</sub>) and axial (**9**<sub>ax</sub>) fluorination was 2:1 in favor of the desired diastereoisomer (**9**<sub>ax</sub>). This hydroxyfluorination also regioselectively installed the C2 OH group, which was then processed to donor **10**.

The union of **10** and the protected amine **11** proceeded with high levels of stereocontrol. The <sup>19</sup>F NMR analysis of **12**

**Scheme 2. Synthesis of the Target Disialoside 2 using the Phosphite Donor 14**


revealed a single peak at  $-218$  ppm, which is fully consistent with  $\alpha$ -selectivity. In contrast,  $^{19}\text{F}$  NMR shifts for the  $\beta$ -anomer typically appear around  $208$ – $209$  ppm.<sup>12</sup> To enable the final glycosylation reaction, the C-8 and C-9 positions of **12** were deprotected using Amberlyst. The resulting product (**13**) was then exposed to phosphite donor **14**.<sup>12</sup> Selective reaction at the primary C-9 position proceeded smoothly and furnished

protected disaccharide **15** with exclusive  $\alpha$ -selectivity. Final deprotection was achieved by exposure to palladium on charcoal, followed by ester hydrolysis, to yield target compound **2** (Scheme 2).

Detailed  $^{19}\text{F}$ -NMR analysis of **2** confirmed the  $\alpha$ -configurations of both linkages, and this was further supported by  $^1\text{H}$  NMR and 2D analysis (Figure 2. Please also see the Supporting Information).

**2.2. In Vivo Validation of Vaccine Candidates in Mice.**

Carbohydrates are known to produce a short-lived and comparatively weak immune response, as they elicit a T-cell-independent response.<sup>25,18</sup> Therefore, to enable T-cell-dependent B-cell activation and impart long-term immunity, glycans are frequently conjugated to a carrier protein.<sup>25,19</sup> Consequently, fluorinated disialoside **2** (DisAF) was covalently conjugated to CRM197, a commonly used and FDA-approved protein in glycoconjugate vaccines,<sup>20</sup> and Porin A, a specific protein from *N. meningitidis* serogroup B.<sup>21</sup> These carrier proteins were linked to the synthetic glycan using a *p*-nitrophenyl adipate ester as a coupling reagent, generating the semisynthetic glycoconjugates DisAF-CRM197, as a MenC vaccine lead, and DisAF-PorA as a bivalent vaccine against both serogroups (Figure 3A).

Two different adjuvants were used in this study: aluminum hydroxide adjuvant (Alum) or Freund's Adjuvant, to compare their effects on the immune response. Alum is an approved and widely employed adjuvant in current human vaccines<sup>22</sup> and Freund's Adjuvant is one of the most widely employed immunopotentiators in animal research.<sup>23a,b</sup>

To determine the immunogenicity of these formulations, four groups of C57BL/6 mice (Envigo,  $n = 6$ ) were immunized with DisAF-CRM-Alum, DisAF-CRM-Freund's, DisAF-PorA-Alum, or DisAF-PorA-Freund's and two control groups ( $n = 6$ ) were injected with PBS-Alum or PBS-Freund's. According to the immunization scheme shown in Figure 3B,  $1\ \mu\text{g}$  of DisAF conjugates in a volume of  $100\ \mu\text{L}$  were injected on days 0, 14,

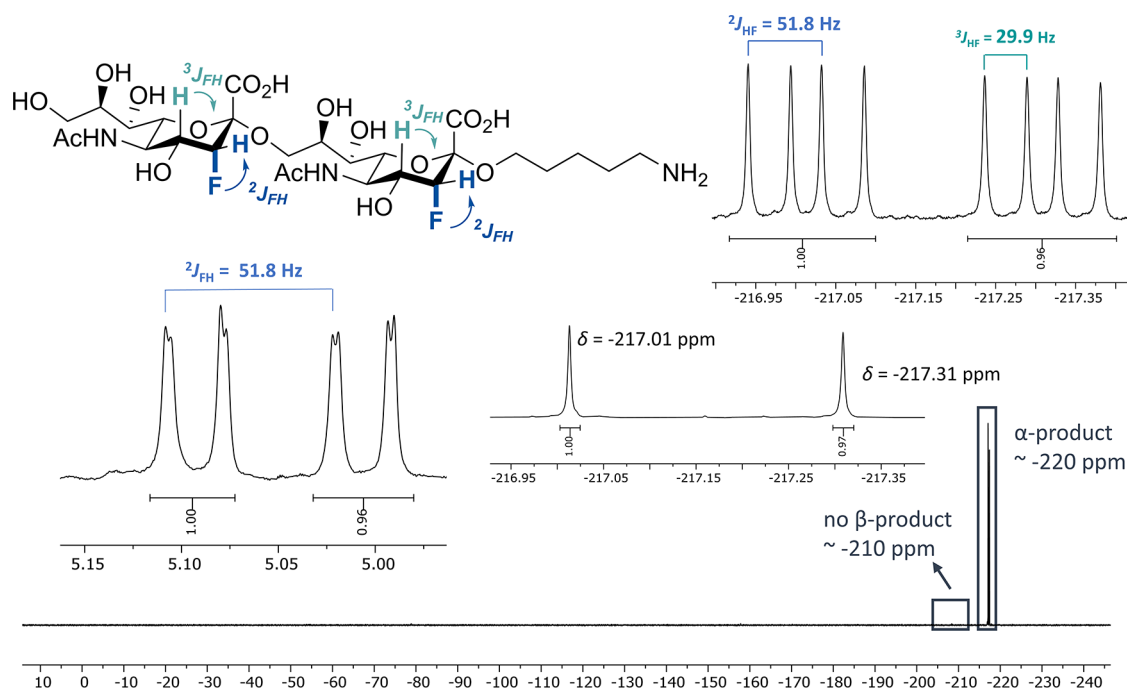


**Figure 2.**  $^{19}\text{F}$  NMR analysis of disialoside **2** (DisAF). Highlighted are the characteristic coupling constants via two and three bonds, respectively.

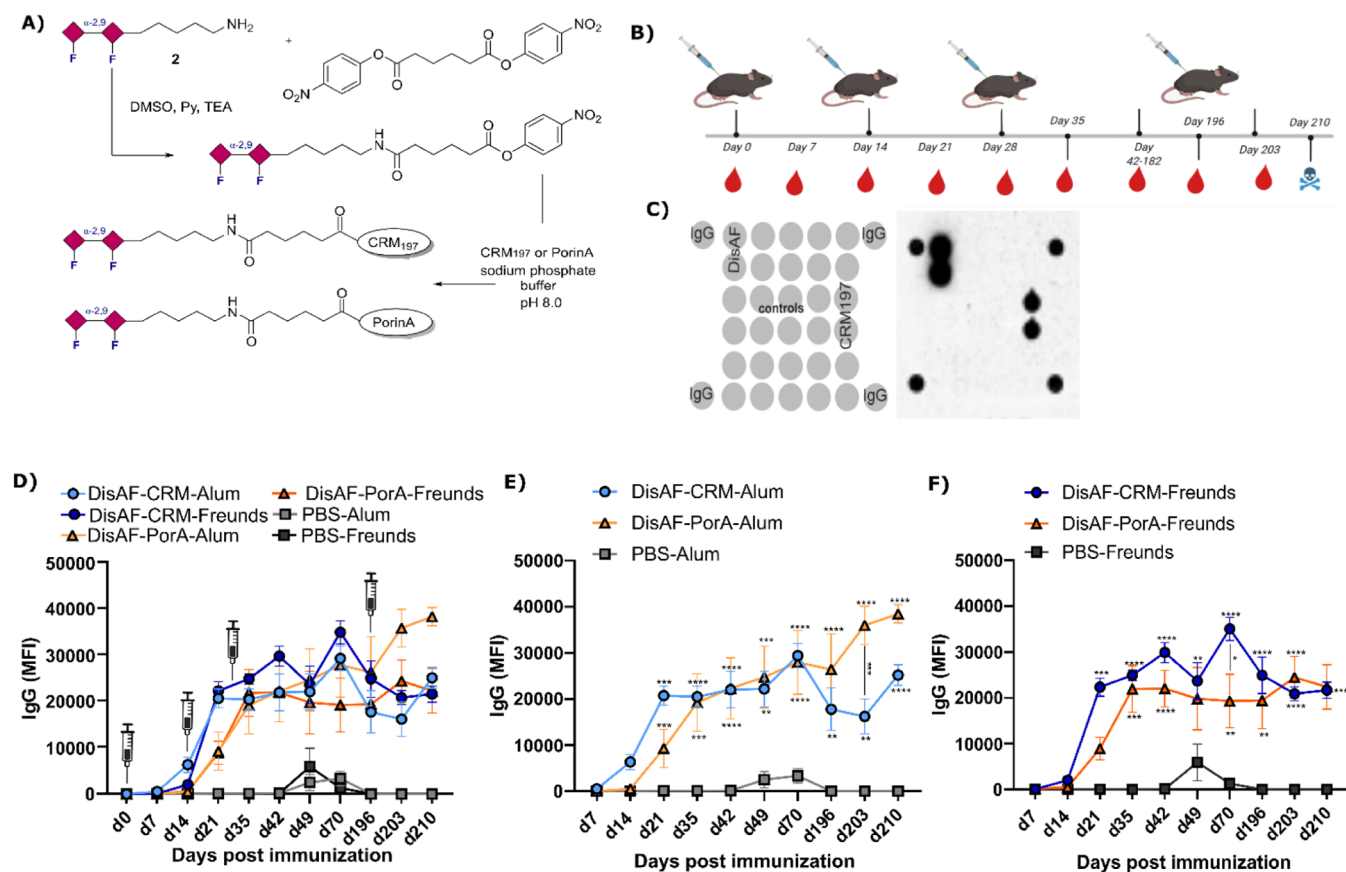


**Figure 3.** All glycoconjugates showed high immunogenicity. A) Fluorinated disaccharide (2, DisAF) and CRM197 or PorA conjugation reactions. B) Immunization schedule. DisAF-CRM-Alum, DisAF-CRM-Freund's, DisAF-PorA-Alum, DisAF-PorA-Freund's, PBS-Alum, and PBS-Freund's were administered at the time points indicated (d0, d14, d28, and d196). Mice ( $n = 6$ ) were immunized with a dose of vaccine equivalent to  $1 \mu\text{g}$  of synthetic antigen. C) A representative picture of the glycan array analysis of serum from immunized mice. The black dots showed the binding of the antibody to DisAF and to CRM197 printed on the glass slide. D) DisAF-specific IgG response measured using glycan arrays. Serum samples from immunized mice were collected at each time point. A serum dilution of 1:100 was used. The different symbols indicate the mean fluorescence intensity value  $\pm$  SEM of six animals per group. E) Evaluation of DisAF-specific IgG response in mice immunized with DisAF-CRM-Alum, DisAF-PorA-Alum, and PBS-Alum was measured by glycan array. The different symbols indicate the mean fluorescence intensity value  $\pm$  SEM of six animals per group. Statistical analysis was performed by Tukey's multiple comparisons test. \*  $p < 0.05$ , \*\*  $p < 0.01$ , \*\*\*  $p < 0.001$ , \*\*\*\*  $p < 0.0001$ . F) The DisAF-specific IgG response in mice immunized with DisAF-CRM-Freund's, DisAF-PorA-Freund's, and PBS-Freund's was measured by a glycan array. The different symbols indicate the mean fluorescence intensity value  $\pm$  SEM of six animals per group. Statistical analysis was performed by Tukey's multiple comparisons test. \*  $p < 0.05$ , \*\*  $p < 0.01$ , \*\*\*  $p < 0.001$ , \*\*\*\*  $p < 0.0001$ .

and 28 and boosted on day 196 to study the long-term immune response. Due to the expected enhanced immune response of the fluorinated carbohydrate relative to the natural epitope,<sup>26g</sup> a significantly lower amount of conjugate was administered than in other studies.<sup>23c</sup>

Glycan arrays allow for simultaneous screening of multiple samples and antigens and facilitate the investigation of specific antibody generation.<sup>24</sup> This approach enabled sera from different mice to be screened to detect antibody levels after immunization. Immunization with all glycoconjugates resulted in antibody production after the second boost, and antibody titers increased over time (Figure 3D–F). All glycoconjugates showed similar IgG long-term responses, meaning that the conjugation to either carrier protein and both adjuvants successfully activated the immune system in a T-cell-dependent manner (Figure 3D). On day 70, the antibody titers reached the highest level and decreased thereafter. Following the last boost on day 196, the IgG levels rose to similar or even higher numbers, indicating that memory B cells were produced that ensure a fast release of high antibody titers.<sup>25</sup> The groups

immunized with DisAF-PorA-Alum and DisAF-CRM-Freund's showed the highest IgG signals (Figure 3E,F). It should be noted that higher antibody titers do not always correlate with higher protection.<sup>26</sup> The different subclasses of IgG, IgG1, IgG2, and IgG3 are related to the level of protection and bacterial clearance.<sup>27</sup> Subclass IgG1 was most prevalent, followed by IgG2 and IgG3 (Figure S3). This finding is in agreement with an earlier study exploring semisynthetic glycoconjugate vaccines against *N. meningitidis*.<sup>14b,28</sup> IgG1 and IgG3 isotypes are very effective in the binding and activation of complement.<sup>29</sup>

IgG1 is well-known to play an important role in opsonization and in effector functions.<sup>30</sup> In addition, it has been determined that murine IgG3 is highly protective, but IgG2 binds strongest to Fc receptors.<sup>26b,27</sup> Therefore, the generation of diverse IgG isotypes can be advantageous against bacteria. The choice of adjuvant can have an effect on the IgG subclasses production.<sup>31</sup> In this investigation, both adjuvants induced a strong production of IgG1 but Alum elicited a



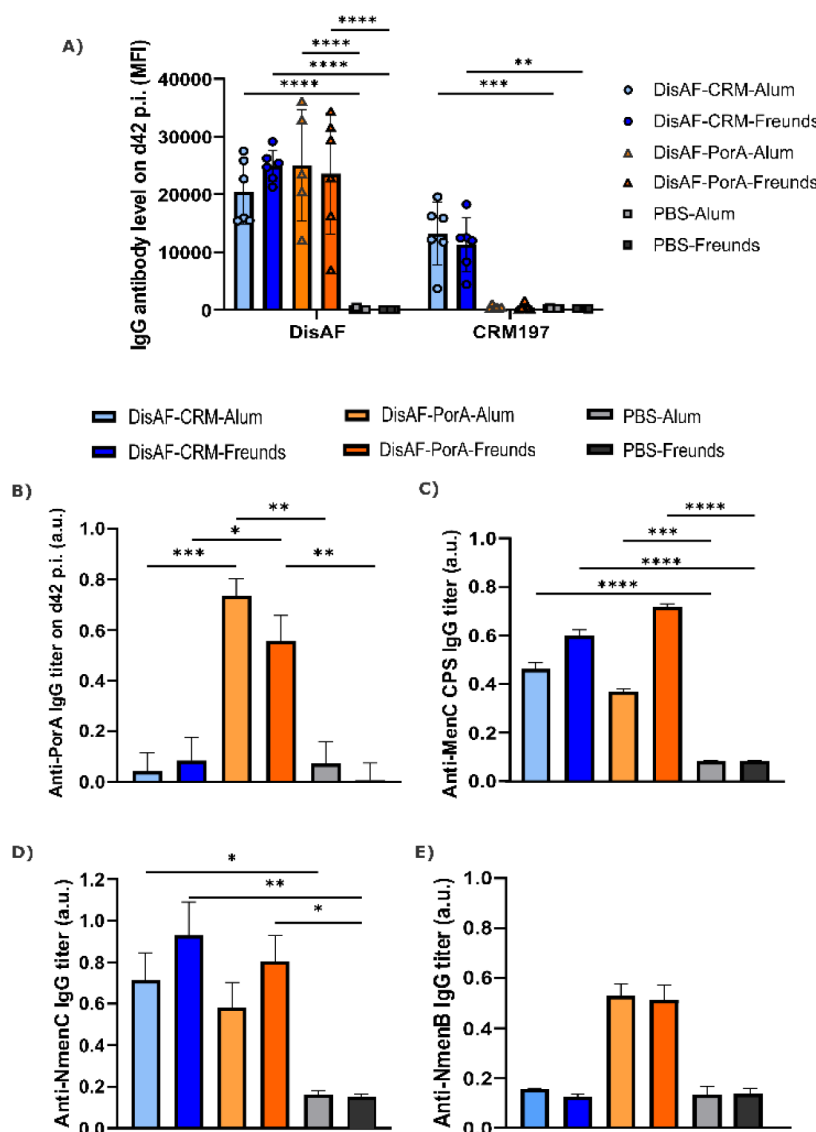


**Figure 4.** Antibodies produced by immunization with different glycoconjugates bind the synthetic glycan, as well as to the native CPS and whole bacteria. A) IgG levels on day 42 postimmunization to the fluorinated glycan and to the carrier protein measured by glycan array. Statistical analysis was performed by Tukey's multiple comparisons test. A serum dilution of 1:100 was used. The different symbols indicate the mean fluorescence intensity value  $\pm$  SEM of six animals per group. \*  $p < 0.05$ , \*\*  $p < 0.01$ , \*\*\*  $p < 0.001$ , \*\*\*\*  $p < 0.0001$ . B) IgG response on d42 p.i. to Porin A in ELISA (Mean  $\pm$  SEM). Statistical analysis was performed by Tukey's multiple comparisons test. A serum dilution of 1:100 was used. \*  $p < 0.05$ , \*\*  $p < 0.01$ , \*\*\*  $p < 0.001$ , \*\*\*\*  $p < 0.0001$ . C) IgG antibody levels were measured using ELISA plates coated with CPS of *N. meningitidis* C (mean  $\pm$  SEM). Statistical analysis was performed by Tukey's multiple comparisons test. A serum dilution of 1:100 was used. \*  $p < 0.05$ , \*\*  $p < 0.01$ , \*\*\*  $p < 0.001$ , \*\*\*\*  $p < 0.0001$ . D) IgG antibody levels were measured using ELISA plates coated with whole *N. meningitidis* C (Mean  $\pm$  SEM). Statistical analysis was performed by Tukey's multiple comparisons test. A serum dilution of 1:100 was used. \*  $p < 0.05$ , \*\*  $p < 0.01$ , \*\*\*  $p < 0.001$ , \*\*\*\*  $p < 0.0001$ . E) IgG antibody levels were measured using ELISA plates coated with whole *N. meningitidis* B (Mean  $\pm$  SEM). Statistical analysis was performed by Tukey's multiple comparisons test (not significant). A serum dilution of 1:100 was used.

higher IgG2 concentration than Freund's adjuvant (Figure S3, see the ESI).

In order to compare the total IgG antibody levels produced by the different groups, the immune responses on day 42 postimmunization were studied in more detail (Figure 4A). In contrast to the negative controls (PBS + Alum or PBS + Freund's Adjuvant), all groups receiving one of the glycoconjugate vaccines responded statistically higher and all showed similar IgG titers. Moreover, the immune response to both carrier proteins was evaluated (Figure 4A,B). The mice immunized with the glycoconjugates produced IgG antibodies that specifically recognized CRM-197 or PorA, respectively,

since carrier proteins can also be presented via MHC II without the attached glycan.<sup>32</sup> Antibody binding and recognition were then tested against the synthetic glycan, the carrier proteins, the native CPS of *N. meningitidis* C (as DisAF mimics its structure), as well as to whole bacteria. The CPS or the whole bacteria were coated on 96-well plates, and the antibody binding was measured by ELISA. Binding was detected in the case of mice vaccinated with the different glycoconjugate formulations (Figure 4C).

Administration of all glycoconjugates led to the production of antibodies that specifically bound to native *N. meningitidis* C

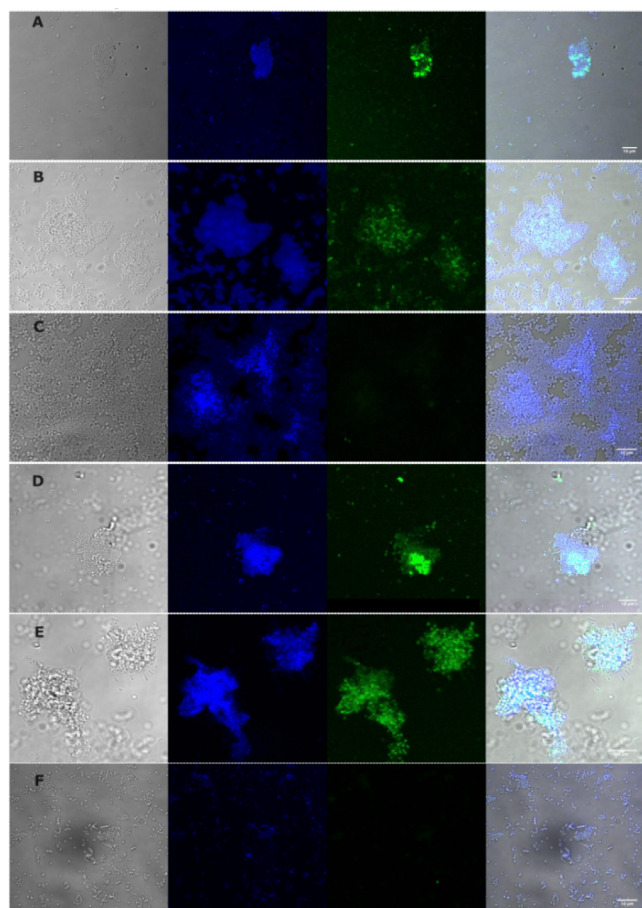


**Figure 5.** Confocal fluorescence microscope images of heat-inactivated *N. meningitidis* with the sera of immunized mice. Green, anti-IgG-488; blue, DAPI; grayscale, transmission light. A) Binding of 1:100 diluted sera of mice immunized with DisAF-CRM-Alum to *N. meningitidis* C. B) Binding of 1:100 diluted sera of mice immunized with DisAF-PorA-Alum to *N. meningitidis* C. C) Binding of 1:100 diluted sera of mice immunized with PBS-Alum to *N. meningitidis* C. D) Binding of 1:100 diluted sera of mice immunized with DisAF-PorA-Alum to *N. meningitidis* B. E) Binding of 1:100 diluted sera of mice immunized with DisAF-PorA-Freund's to *N. meningitidis* B. F) Binding of 1:100 diluted sera of mice immunized with PBS-Freund's to *N. meningitidis* B.

CPS (Figure 4C). The response by the groups receiving Freund's Adjuvant was slightly but not significantly higher.

A higher production of binding antibodies might influence protection efficacy, but this is not directly linked.<sup>26b,31</sup> It is interesting to note that the antibodies were also bound to whole bacteria (Figure 4D). Only mice immunized with glycoconjugates containing PorA as carrier proteins generated antibodies that specifically recognized *N. meningitidis* B (Figure 4E).

Confocal fluorescence microscopy confirmed that the antibodies recognize native CPS on the surface of the bacteria. The pooled sera from the different groups of mice were incubated with heat-inactivated *N. meningitidis* C or *N. meningitidis* B, respectively, and labeled with anti-IgG-488. Animals immunized with the synthetic glycan exhibited strong binding of IgG to *N. meningitidis* C (Figures 5A,B and S4). However, no signal was detected in the negative controls (Figures 5C and S4). Moreover, the antibodies generated by mice immunized with glycoconjugates that contained PorA

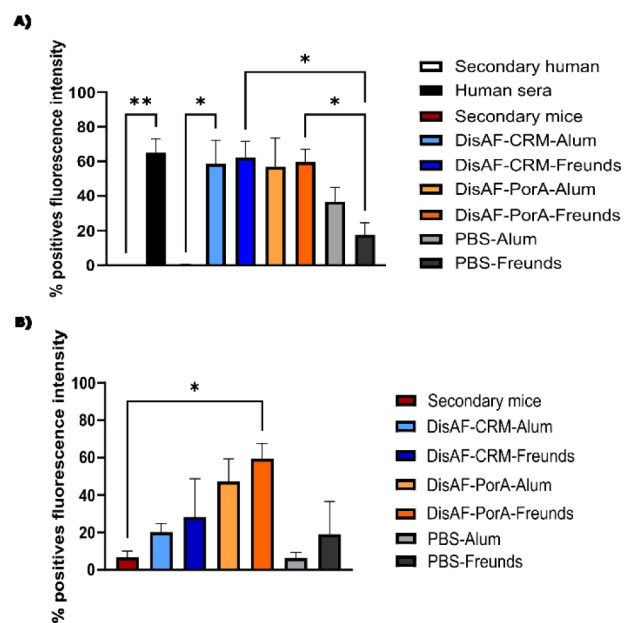


**Figure 6.** Quantification of flow cytometry-binding assays. A) Binding of 1:100 diluted sera and controls to *N. meningitidis* C ( $n = 3$ ). B) Binding of 1:100 diluted sera and controls to *N. meningitidis* B ( $n = 3$ ).

recognized *N. meningitidis* B (Figures 5D,E and S5). Nonetheless, no binding was observed in either the negative controls or the groups with CRM197 as the carrier protein (Figure S4). Hence, conjugating the glycan to PorA, which is specific for *N. meningitidis* B, resulted in the generation of antibodies that bound to both serogroups. These findings were consistent with the results obtained by the ELISA.

The binding of serum antibodies to the respective bacteria was quantified using flow cytometry. Sera dilutions of 1:100 were incubated with  $10^7$  CFU/mL of bacteria and labeled with anti-IgG-488. Before quantification, samples were fixed with 4% PFA. Antibodies produced by all of the groups receiving the glycoconjugate were bound to *N. meningitidis* C, while none of the negative controls were bound (Figure 6A). Moreover, the groups immunized with PorA as a carrier protein produced antibodies that bound to *N. meningitidis* B (Figure 6B). Some unspecific binding in the negative control groups was observed.<sup>33</sup> The different techniques, ELISA, confocal fluorescence microscopy, and flow cytometry, demonstrated that the antibodies generated in response to the immunization with glycoconjugates bound to the bacterial cell wall as they recognized native CPS.

The antibodies strongly bound to the pathogen, but their key role is to eliminate the bacteria and protect against infection.<sup>34</sup> Two *in vitro* functional assays were employed to assess the functional activity of the antibodies and measure the vaccine efficacy,<sup>35</sup> the serum bactericidal antibody (SBA) assay and the opsonophagocytic killing assay (OPKA). Both assays work similarly, whereas, SBA mediates antibody-mediated and complement-dependent killing of the bacteria, OPKA measures antibody-mediated, complement-dependent uptake and killing by phagocytic cells.<sup>35</sup> The SBA assay was performed with either *N. meningitidis* B or C using the rabbit complement. Sera from humans vaccinated against *N. meningitidis* C served as a positive control.

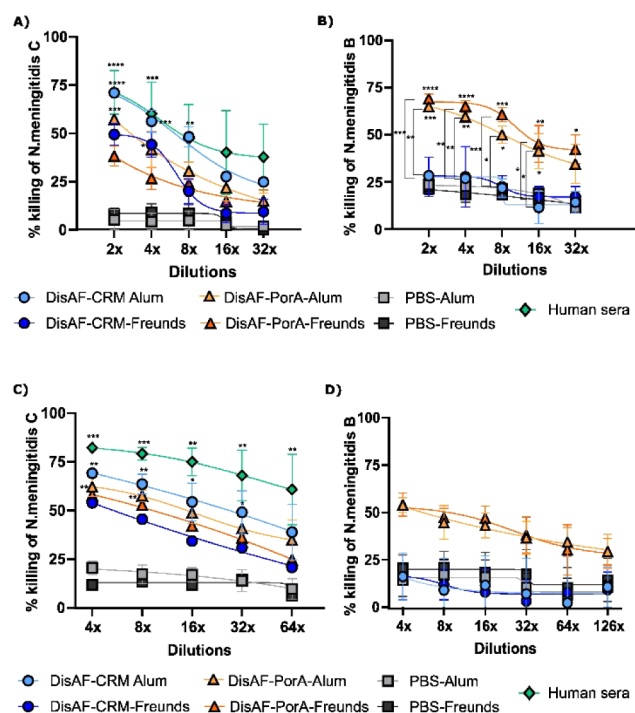


**Figure 7.** *In vitro* killing activity of DisAF-CRM-Alum, DisAF-CRM-Freund's, DisAF-PorA-Alum, DisAF-PorA-Freund's, and PBS-Alum and PBS-Freund's vaccine-generated antibodies. A) Serum bactericidal assay. *In vitro* complement killing of *N. meningitidis* C mediated by polyclonal antibodies from the immunized mice ( $n = 6$ ). Data are means of CFU reduction relative to negative control wells (samples lacking antibodies) of three independent experiments. Human control sera from immunized patients were used as a standard. B) Serum bactericidal assay. *In vitro* complement killing of *N. meningitidis* B mediated by polyclonal antibodies from the immunized mice ( $n = 6$ ). Data are means of CFU reduction relative to negative control wells (samples lacking antibodies) of three independent experiments. C) Opsonophagocytic killing assay. *In vitro* opsonophagocytic killing of *N. meningitidis* C mediated by polyclonal antibodies from the immunized mice ( $n = 6$ ). Data are means of CFU reduction relative to negative control wells (samples lacking antibodies) of three independent experiments. Human control sera from vaccinated patients against *N. meningitidis* C were used as a standard. D) Opsonophagocytic killing assay. *In vitro* opsonophagocytic killing of *N. meningitidis* B mediated by polyclonal antibodies from the immunized mice ( $n = 6$ ). Data are means of CFU reduction relative to negative control wells (samples lacking antibody) of three independent experiments.

We observed that in both DisAF-CRM-Alum and the human sera control at a 1:8 sera dilution, there is 50% killing of *N. meningitidis* C (Figure 7A), similar to previous reports using synthetic glycan-based vaccine candidates.<sup>28,36</sup> For the other groups, 50% killing occurs at a 1:4 dilution (Figure 7A). Only antibodies produced by the animals that received PorA as the carrier protein are protective against *N. meningitidis* B, with 50% killing at a 1:8 dilution (Figure 7B). Antibodies from the group that received DisAF-CRM-Alum display the highest level of protection, but the group receiving DisAF-PorA-Alum appears to be protective against both *N. meningitidis* B and C.

OPKA quantifies the opsonic activity of the specific antibodies and the uptake of the bacteria by phagocytic cells, resulting in the death of the bacteria.<sup>29a,35</sup> The 50% killing of *N. meningitidis* C is between 1:32 and 1:64 serum dilutions for the DisAF-CRM-Alum group, but human control sera showed

a slightly higher protection (Figure 7C). For the other groups, the 50% killing of *N. meningitidis* C and the 50% killing of *N. meningitidis* B occurred at a serum dilution of 1:16 (Figure 7C,D). As for SBA, the DisAF-CRM-Alum group elicits the strongest protection against *N. meningitidis* C, and DisAF-PorA-Alum antibodies are somewhat protective against both serogroups.

These results indicate that although the groups that received Freund's Adjuvant may produce slightly higher levels of IgG antibodies, it does not necessarily imply that these antibodies are more effective in providing protection.<sup>26b,31</sup> The group immunized with DisAF-CRM-Alum was most effectively protected, while the antibodies produced by the DisAF-PorA-Alum group were able to provide some protection against both serogroups. Both groups showed higher signals of IgG1 and IgG2, which may be essential in fighting the pathogen, as they play a crucial role in opsonization as well as in effector functions.<sup>29,30</sup> IgG2 is known to be involved in anticarbohydrate responses against bacterial capsular polysaccharides.<sup>37</sup> It is important to stress that the complexity of the immune system implicates other factors, such as inflammatory responses or complement recruitment, in providing protection.<sup>27,31</sup>

### 3. CONCLUSION

In conclusion, a synthetic, difluorinated glycomimetic of the  $\alpha$ -(2,9)-sialyl epitope (2, DisAF) of *N. meningitidis* C was produced in 16 steps. Stereoselective chemical sialylation proved to be key in the assembly of the lead structure, where the directing effect of the  $C(sp^3)$ -F bond enabled the target  $\alpha$ -disialoside to be forged efficiently and suppressed competing elimination. This chemical strategy enables configurationally well-defined material to be accessed on a large scale, and mitigates many of the risks associated with material isolated from biological sources. The fluorinated mimics are excellent bioisosteres of the native system and induce the generation of highly specific IgG antibodies. To achieve a T-cell-dependent immune response and enhance the generation of memory B cells, the fluorinated glycan was conjugated to the carrier proteins, CRM-197 or PorA. All glycoconjugates induced a strong and long-lasting IgG response, as IgG1 dominated in mice. Varying the carrier proteins or adjuvants did not result in notable differences in the antibody response. A key feature of this design is that the combination of the fluorinated glycan epitope of MenC with an outer cell membrane protein of MenB enables the generation of a bivalent vaccine against both serogroups. PorA glycoconjugates induced the production of strong binding antibodies to *N. meningitidis* C and *N. meningitidis* B, indicating that these fluorinated glycoconjugates are promising vaccine leads against *N. meningitidis* serogroups B and/or C.

### ASSOCIATED CONTENT

#### Supporting Information

The Supporting Information is available free of charge at <https://pubs.acs.org/doi/10.1021/jacs.4c03179>.

Supplementary tables and figures, full experimental procedures and analytical data ( $^1H$ ,  $^{13}C$ , and  $^{19}F$  spectral data) for new compounds (PDF)



## AUTHOR INFORMATION

### Corresponding Authors

**Peter H. Seeberger** – Department of Biomolecular Systems, Max Planck Institute for Colloids and Interfaces, Potsdam 14476, Germany; Freie Universität Berlin, Institute of Chemistry and Biochemistry, Berlin 14195, Germany; [orcid.org/0000-0003-3394-8466](https://orcid.org/0000-0003-3394-8466);  
Email: [Peter.Seeberger@mpikg.mpg.de](mailto:Peter.Seeberger@mpikg.mpg.de)

**Ryan Gilmour** – Institute for Organic Chemistry, University of Münster, Münster 48149, Germany; [orcid.org/0000-0002-3153-6065](https://orcid.org/0000-0002-3153-6065); Email: [ryan.gilmour@uni-muenster.de](mailto:ryan.gilmour@uni-muenster.de)

### Authors

**Christina Jordan** – Institute for Organic Chemistry, University of Münster, Münster 48149, Germany

**Kathrin Siebold** – Institute for Organic Chemistry, University of Münster, Münster 48149, Germany

**Patricia Priegue** – Department of Biomolecular Systems, Max Planck Institute for Colloids and Interfaces, Potsdam 14476, Germany; Freie Universität Berlin, Institute of Chemistry and Biochemistry, Berlin 14195, Germany

Complete contact information is available at:

<https://pubs.acs.org/10.1021/jacs.4c03179>

### Author Contributions

<sup>#</sup>C.J., K.S., and P.P. contributed equally to this work. The manuscript was written through contributions of all authors. All authors have given approval to the final version of the manuscript.

### Notes

The authors declare no competing financial interest.

## ACKNOWLEDGMENTS

We acknowledge generous financial support from the European Research Council (ERC Consolidator Grant 818949), the University of Münster, and the Max Planck Society. We thank Fabienne Weber and Emelie Reuber for their help during the mice immunizations and Dr. Charlotte Teschers for helpful discussions.

## REFERENCES

(1) (a) Sturgis, P.; Brunton-Smith, I.; Jackson, J. Trust in Science, social consensus and vaccine confidence. *Nat. Hum. Behav.* **2021**, *5* (11), 1528–1534. (b) Korn, L.; Böhm, P.; Meier, N. W.; Betsch, C. Vaccination as a social contract. *Proc. Natl. Acad. Sci. U. S. A.* **2020**, *117*, 14890–14899. (c) Fayaz-Farkhad, B.; Jung, H.; Calabrese, C.; Albarracin, D. State policies increase vaccination by shaping social norms. *Sci. Rep.* **2023**, *13* (1), 21277. (d) Tripathi, T. Advances in vaccines: revolutionizing disease prevention. *Sci. Rep.* **2023**, *13* (1), 11748. (2) (a) Danishefsky, S. J.; Allen, J. R. From the Laboratory to the Clinic: A Retrospective on Fully Synthetic Carbohydrate-Based Anticancer Vaccines. *Angew. Chem., Int. Ed.* **2000**, *39* (5), 836–863. (b) Danishefsky, S. J.; Shue, Y.-K.; Chang, M. N.; Wong, C.-H. Development of Globo-H Cancer Vaccine. *Acc. Chem. Res.* **2015**, *48*, 643–652. (c) Hecht, M.-L.; Stallforth, P.; Varoón-Silva, D.; Adibekian, A.; Seeberger, P. H. Recent advances in carbohydrate-based vaccines. *Curr. Opin. Chem. Biol.* **2009**, *13* (3), 354–359. (d) Astronomo, R. D.; Burton, D. R. Carbohydrate vaccines: developing sweet solutions to sticky situation. *Nat. Rev. Drug Discovery* **2010**, *9*, 308–324. (e) Hoffmann-Röder, A.; Kaiser, A.; Wagner, S.; Gaidzik, N.; Kowalczyk, D.; Westerlind, U.; Gerlitzki, B.; Schmitt, E.; Kunz, H. Synthetic antitumor vaccines from tetanus toxoid conjugates of MUC1 glycopeptides with the Thomsen-

Friedenreich antigen and a fluorine-substituted analogue. *Angew. Chem., Int. Ed.* **2010**, *49*, 8498–8503. (f) Yang, F.; Zheng, X.-J.; Huo, C.-X.; Wang, Y.; Zhang, Y.; Ye, X.-S. Enhancement of the Immunogenicity of Synthetic Carbohydrate Vaccines by Chemical Modifications of STn Antigen. *ACS Chem. Biol.* **2011**, *6*, 252–259. (g) Lee, H.-Y.; Chen, C.-Y.; Tsai, T.-I.; Li, S.-T.; Lin, K.-H.; Cheng, Y.-Y.; Ren, C.-T.; Cheng, T.-J. R.; Wu, T.-J. R.; Wong, C.-H. Immunogenicity Study of Globo H Analogues with Modification at the Reducing or Nonreducing End of the Tumor Antigen. *J. Am. Chem. Soc.* **2014**, *136* (48), 16844–16853. (h) Seeberger, P. H. Discovery of Semi- and Fully-Synthetic Carbohydrate Vaccines Against Bacterial Infections Using a Medicinal Chemistry Approach. *Chem. Rev.* **2021**, *121*, 3598–3626. (i) Del Bino, L.; Østerlid, K. E.; Wu, D.-Y.; Nonne, F.; Romano, M. R.; Codée, J.; Adamo, R. Synthetic Glycans to Improve Current Glycoconjugate Vaccines and Fight Antimicrobial Resistance. *Chem. Rev.* **2022**, *122*, 15672–15716. (j) Shivatare, S. S.; Shivatare, V. S.; Wong, C.-H. Glycoconjugates: Synthesis, Functional Studies, and Therapeutic Developments. *Chem. Rev.* **2022**, *122*, 15603–15671. (k) Mahmoud, A.; Toth, I.; Stephenson, R. Developing an Effective Glycan-Based Vaccine for *Streptococcus Pyogenes*. *Angew. Chem., Int. Ed.* **2022**, *61* (11), No. e202115342.

(3) Werz, D. B.; Ranzinger, R.; Herget, S.; Adibekian, A.; von der Lieth, C.-W.; Seeberger, P. H. Exploring the Structural Diversity of Mammalian Carbohydrates (“Glycospace”) by Statistical Databank Analysis. *ACS Chem. Biol.* **2007**, *2* (10), 685–691.

(4) (a) Varki, A. Biological Roles of oligosaccharides: all of the theories are correct. *Glycobiology* **1993**, *3* (2), 97–130. (b) Bertozzi, C. R.; Kiessling, L. L. Chemical Glycobiology. *Science* **2001**, *291*, 2357–2364. (c) Nowack, L.; Teschers, C. S.; Albrecht, S.; Gilmour, R. Oligodendroglial Glycolipids in (Re) Myelination: Implications for Multiple Sclerosis Research. *Nat. Prod. Rep.* **2021**, *38*, 890–904. (d) Varki, A.; Cummings, R. D.; Esko, J. D.; Stanley, P.; Hart, G. W.; Aebi, M.; Mohnen, D.; Kinoshita, T.; Packer, N. H.; Prestegard, J. H., et al. *Essentials of Glycobiology*, 4th ed.; Cold Spring Harbor Laboratory Press: Cold Spring Harbor, NY, 2022.

(5) (a) Lasky, L. A. Selectins: interpreters of cell-specific carbohydrate information during inflammation. *Science* **1992**, *258* (5084), 964–969. (b) Lee, Y. C.; Lee, R. T. Carbohydrate-Protein Interactions: Basis of Glycobiology. *Acc. Chem. Res.* **1995**, *28*, 321–327. (c) Dwek, R. A. Glycobiology: Towards Understanding the Function of Sugars. *Chem. Rev.* **1996**, *96*, 683–720. (d) van Kooyk, Y.; Rabinovich, G. A. Protein-Glycan interactions in the control of innate and adaptive immune responses. *Nat. Immunol.* **2008**, *9*, 593–601. (e) Ernst, B.; Magnani, J. L. From carbohydrate leads to glycomimetic drugs. *Nat. Rev. Drug Discovery* **2009**, *8*, 661–677. (f) Magnani, J. L.; Ernst, B. Glycomimetic Drugs – a new source of therapeutic opportunities. *Discovery Med.* **2009**, *8*, 247–252. (g) Reina, J. J.; Bernardi, A. Carbohydrate mimics and lectins: a source of new drugs and therapeutic opportunities. *Mini-Rev. Med. Chem.* **2012**, *12* (14), 1434–1442. (h) Leusmann, S.; Ménová, P.; Shanin, E.; Titz, A.; Rademacher, C. Glycomimetics for the inhibition and modulation of lectins. *Chem. Soc. Rev.* **2023**, *52*, 3663–3740.

(6) (a) Street, I. P.; Kempton, J. B.; Withers, S. G. Inactivation of a  $\beta$ -3-Glucosidase through the Accumulation of a Stable 2-Deoxy-2-fluoro- $\alpha$ -D-glucopyranosyl-Enzyme Intermediate: A Detailed Investigation. *Biochemistry* **1992**, *31* (41), 9970–9978. (b) Zechel, D. L.; Withers, S. G. Glycosidase mechanisms: anatomy of a finely tuned catalyst. *Acc. Chem. Res.* **2000**, *33*, 11–18.

(7) (a) Watts, A. G.; Damager, I.; Amaya, M. L.; Buschiazio, A.; Alzari, P.; Frasc, A. C.; Withers, S. G. Trypanosoma cruzi Transsialidase Operates through a Covalent Sialyl-Enzyme Intermediate: Tyrosine Is the Catalytic Nucleophile. *J. Am. Chem. Soc.* **2003**, *125* (25), 7532. (b) Tsai, C.-S.; Yen, H.-Y.; Lin, M.-I.; Tsai, T.-I.; Wang, S.-Y.; Huang, W.-I.; Hsu, T.-L.; Cheng, Y.-S. E.; Fang, J.-M.; Wong, C.-H. Cell-permeable probe for identification and imaging of sialidases. *Proc. Natl. Acad. Sci. U. S. A.* **2013**, *110*, 2466. (c) Weck, S.; Robinson, K.; Smith, M. R.; Withers, S. G. Understanding viral neuraminidase inhibition by substituted difluoroallic acids. *Chem.*



- Commun.* **2015**, *51* (51), 2933. (d) Lo, H.-J.; Krasnova, L.; Dey, S.; Cheng, T.; Liu, H.; Tsai, T.-I.; Wu, K. B.; Wu, C.-Y.; Wong, C.-H. Synthesis of Sialidase-Resistant Oligosaccharide and Antibody Glycoform Containing  $\alpha$ 2,6-Linked 3F<sup>XX</sup>-Neu5Ac. *J. Am. Chem. Soc.* **2019**, *141*, 6484–6488. (e) Axer, A.; Jumde, R. P.; Adam, S.; Faust, A.; Schäfers, M.; Fobker, M.; Koehnke, J.; Hirsch, A. K. H.; Gilmour, R. Enhancing Glycan Stability via Site-Selective Fluorination: Modulating Substrate Orientation by Molecular Design. *Chem. Sci.* **2021**, *12*, 1286–1294.
- (8) Streety, X. S.; Obike, J. C.; Townsend, S. D. A Hitchhiker's Guide to Problem Selection in Carbohydrate Synthesis. *ACS Cent. Sci.* **2023**, *9*, 1285–1296.
- (9) (a) Müller, K.; Faeh, C.; Diederich, F. Fluorine in Pharmaceuticals: Looking Beyond Intuition. *Science* **2007**, *317* (5846), 1881–1886. (b) Shah, P.; Westwell, A. D. The role of fluorine in medicinal chemistry. *J. Enzyme Inhib. Med. Chem.* **2007**, *22*, 527–540. (c) O'Hagan, D. Fluorine in health care: Organofluorine containing blockbuster drugs. *J. Fluorine Chem.* **2010**, *131*, 1071–1081. (d) Meanwell, N. A. Fluorine and fluorinated motifs in the design and application of bioisosteres for drug design. *J. Med. Chem.* **2018**, *61*, 5822–5880.
- (10) (a) Bucher, C.; Gilmour, R. Fluorine-Directed Glycosylation. *Angew. Chem., Int. Ed.* **2010**, *49* (46), 8724–8728. (b) Durantie, E.; Bucher, C.; Gilmour, R. Fluorine-Directed  $\beta$ -Galactosylation: Chemical Glycosylation Development by Molecular Editing. *Chem. — Eur. J.* **2012**, *18*, 8208–8215. (c) Santschi, N.; Gilmour, R. Comparative Analysis of Fluorine-Directed Glycosylation Selectivity: Interrogating C2 [OH  $\rightarrow$  F] Substitution in d-Glucose and d-Galactose. *Eur. J. Org. Chem.* **2015**, *2015* (32), 6983–6987. (d) Kieser, T. J.; Santschi, N.; Nowack, L.; Kehr, G.; Kuhlmann, T.; Albrecht, S.; Gilmour, R. Single Site Fluorination of the GM4 Ganglioside Epitope Upregulates Oligodendrocyte Differentiation. *ACS Chem. Neurosci.* **2018**, *9*, 1159–1165. (e) Teschers, C. S.; Gilmour, R. Fluorine-Directed Mannoside Assembly. *Angew. Chem., Int. Ed.* **2023**, *135* (3), No. e202213304.
- (11) (a) Chen, H.; Viel, S.; Ziarelli, F.; Peng, L. <sup>19</sup>F NMR: a valuable tool for studying biological events. *Chem. Soc. Rev.* **2013**, *42* (20), 7971–7982. (b) Rosenau, C. P.; Jelier, B. J.; Gossert, A. D.; Togni, A. Exposing the Origins of Irreproducibility in Fluorine NMR Spectroscopy. *Angew. Chem., Int. Ed.* **2018**, *57*, 9528–9533. (c) Fittolani, G.; Shanina, E.; Guberman, M.; Seeberger, P. H.; Rademacher, C.; Delbianco, M. Automated Glycan Assembly of <sup>19</sup>F-labeled Glycan Probes Enables High-Throughput NMR Studies of Protein–Glycan Interactions. *Angew. Chem., Int. Ed.* **2021**, *60*, 13302. (d) Dalvit, C.; Gmür, I.; Röbber, P.; Gossert, A. D. Affinity measurement of strong ligands with NMR spectroscopy: Limitations and ways to overcome them. *Prog. Nucl. Magn. Reson. Spectrosc.* **2023**, *138–139*, 52–69.
- (12) (a) Hayashi, T.; Kehr, G.; Bergander, K.; Gilmour, R. Stereospecific  $\alpha$ -Sialylation by Site-Selective Fluorination. *Angew. Chem., Int. Ed.* **2019**, *58* (12), 3814–3818. (b) Hayashi, T.; Axer, A.; Kehr, G.; Bergander, K.; Gilmour, R. Halogen-Directed Chemical Sialylation: Pseudo-Stereodivergent Access to Marine Ganglioside Epitopes. *Chem. Sci.* **2020**, *11*, 6527–6531.
- (13) (a) McCoy, R. D.; Vimr, E. R.; Troy, F. A. CMP-NeuNAc: poly- $\alpha$ -2,8-sialosyl sialyltransferase and the biosynthesis of polysialosyl units in neural cell adhesion molecules. *J. Biol. Chem.* **1985**, *260* (23), 12695. (b) Robbins, J. B.; Schneerson, R.; Xie, G.; Hanson, L. A.; Miller, M. A. Capsular polysaccharide vaccine for Group B: *Neisseria meningitidis*, *Escherichia coli* K1, and *Pasteurella haemolytica* A2. *Proc. Natl. Acad. Sci. U. S. A.* **2011**, *108*, 17871–17875.
- (14) (a) Chu, K.-C.; Ren, C.-T.; Lu, C.-P.; Hsu, C.-H.; Sun, T.-H.; Han, J.-L.; Pal, B.; Chao, T.-A.; Lin, Y.-F.; Wu, S.-H.; et al. Efficient and Stereoselective Synthesis of  $\alpha$ (2 $\rightarrow$ 9) Oligosialic Acids: From Monomers to Dodecamers. *Angew. Chem., Int. Ed.* **2011**, *123* (40), 9563–9567. (b) Liao, G.; Zhou, Z.; Guo, Z. Synthesis and immunological study of  $\alpha$ -2,9-oligosialic acid conjugates as anti-group C meningitis vaccines. *Chem. Commun.* **2015**, *51*, 9647–9650.
- (15) (a) Wu, C.-Y.; Huang, Y.-L. Carbohydrate-based vaccines: challenges and opportunities. *Expert Rev. Vaccines* **2010**, *9* (11), 1257–1274. (b) Bardotti, A.; Averani, G.; Berti, F.; Berti, S.; Carinci, V.; D'Ascenzi, S.; Fabbri, B.; Giannini, S.; Giannozzi, A.; Magagnoli, C.; et al. Physicochemical characterisation of glycoconjugate vaccines for prevention of meningococcal diseases. *Vaccine* **2008**, *26* (18), 2284–2296.
- (16) (a) Boons, G. J.; Demchenko, A. V. Recent Advances in O-Sialylation. *Chem. Rev.* **2000**, *100* (12), 4539–4566. (b) Chen, X.; Varki, A. Advances in the chemistry and biology of sialic acids. *ACS Chem. Biol.* **2010**, *5*, 163–176.
- (17) Burkart, M. D.; Zhang, Z.; Hung, S.-C.; Wong, C.-H. A New Method for the Synthesis of Fluoro-Carbohydrates and Glycosides Using Selectfluor. *J. Am. Chem. Soc.* **1997**, *119*, 11743–11746.
- (18) (a) Zimmermann, S.; Lepenies, B. Glycans as Vaccine Antigens and Adjuvants: Immunological Considerations. In *Carbohydrate-Based Vaccines. Methods in Molecular Biology*; Humana Press, 2015. (b) Zimmermann, S.; Lepenies, B. Glycans as Vaccine Antigens and Adjuvants: Immunological Considerations. *Methods Mol. Biol.* **2015**, *1331*, 11–26. (c) Rajendra Rohokale, R.; Guo, Z. Development in the Concept of Bacterial Polysaccharide Repeating Unit-Based Antibacterial Conjugate Vaccines. *ACS Infect. Dis.* **2023**, *9*, 178–212.
- (19) Adamo, R. Glycoconjugate vaccines: classic and novel approaches. *Glycoconj. J.* **2021**, *38*, 397–398.
- (20) Khatuntseva, E. A.; Nifantiev, N. E. Cross reacting material (CRM197) as a carrier protein for carbohydrate conjugate vaccines targeted at bacterial and fungal pathogens. *Int. J. Biol. Macromol.* **2022**, *218*, 775–798.
- (21) Vermont, C. L.; van Dijken, H. H.; de Groot, R.; van den Dobbelen, G. P. Porin A-specific antibody avidity in patients who are convalescing from meningococcal B disease. *Pediatr. Res.* **2005**, *58*, 149–152.
- (22) Reed, S. G. Vaccine adjuvants. *Expert Rev. Vaccines* **2013**, *12*, 705–706.
- (23) (a) Stils, H. F., Jr. Adjuvants and Antibody Production: Dispelling the Myths Associated with Freund's Complete and Other Adjuvants. *Ilar J.* **2005**, *46* (3), 280–293. (b) Powers, J. G.; Nash, P. B.; Rhyan, J. C.; Yoder, C. A.; Miller, L. A. Comparison of immune and adverse effects induced by AdjuVac and Freund's complete adjuvant in New Zealand white rabbits (*Oryctolagus cuniculus*). *Lab. Anim. (NY)* **2007**, *36*, 51–58. (c) Adamo, R.; Nilo, A.; Harfouche, C.; Brogioni, B.; Pecetta, S.; Brogioni, G.; Balducci, E.; Pinto, V.; Filippini, S.; et al. Investigating the immunodominance of carbohydrate antigens in a bivalent unimolecular glycoconjugate vaccine against serogroup A and C meningococcal disease. *Glycoconj. J.* **2014**, *31*, 637–647.
- (24) (a) Geissner, A.; Seeberger, P. H. Glycan Arrays: From Basic Biochemical Research to Bioanalytical and Biomedical Applications. *Ann. Rev. Anal. Chem.* **2016**, *9* (1), 223–247. (b) Geissner, A.; Reinhardt, A.; Rademacher, C.; Johannsen, T.; Monteiro, J.; Lepenies, B.; Thepaut, M.; Fieschi, F.; Mrazkova, J.; Wimmerova, M.; et al. Microbe-focused glycan array screening platform. *Proc. Natl. Acad. Sci. U. S. A.* **2019**, *116*, 1958–1967. (c) Kaplonek, P.; Seeberger, P. H. Glycan Microarrays Containing Synthetic Streptococcus pneumoniae CPS Fragments and Their Application to Vaccine Development. *Methods Mol. Biol.* **2022**, *2460*, 193–206.
- (25) (a) Castellino, F.; Galli, G.; Del Giudice, G.; Rappuoli, R. Generating memory with vaccination. *Eur. J. Immunol.* **2009**, *39*, 2100–2105. (b) Reinhardt, A.; Yang, Y.; Claus, H.; Pereira, C. L.; Cox, A. D.; Vogel, U.; Anish, C.; Seeberger, P. H. Antigenic potential of a highly conserved *Neisseria meningitidis* lipopolysaccharide inner core structure defined by chemical synthesis. *Chem. Biol.* **2015**, *22*, 38–49.
- (26) (a) Tarrago, D.; Aguilar, L.; Jansen, W. T.; Gimenez, M. J.; Avellon, A.; Granizo, J. J.; Casal, J. Dependence of correlations between antibody titres and opsonophagocytosis on pneumococcal serotype and patient morbidity in pre- and post pneumococcal vaccination states. *Clin. Microbiol. Infect.* **2007**, *13* (4), 369–376. (b) Lofano, G.; Gorman, M. J.; Yousif, A. S.; Yu, W. H.; Fox, J. M.;

Dugast, A. S.; Ackerman, M. E.; Suscovich, T. J.; Weiner, J.; Barouch, D.; et al. Antigen-specific antibody Fc glycosylation enhances humoral immunity via the recruitment of complement. *Sci. Immunol.* **2018**, *3* (26), No. eaat7796. (c) Fischinger, S.; Fallon, J. K.; Michell, A. R.; Broge, T.; Suscovich, T. J.; Streeck, H.; Alter, G. A high-throughput, bead-based, antigen-specific assay to assess the ability of antibodies to induce complement activation. *J. Immunol. Methods* **2019**, *473*, 112630.

(27) Michaelsen, T. E.; Kolberg, J.; Aase, A.; Herstad, T. K.; Hoiby, E. A. The four mouse IgG isotypes differ extensively in bactericidal and opsonophagocytic activity when reacting with the P1.16 epitope on the outer membrane PorA protein of *Neisseria meningitidis*. *Scand. J. Immunol.* **2004**, *59*, 34–39.

(28) Liao, G.; Zhou, Z.; Suryawanshi, S.; Mondal, M. A.; Guo, Z. Fully Synthetic Self-Adjuvanting alpha-2,9-Oligosialic Acid Based Conjugate Vaccines against Group C Meningitis. *ACS Cent. Sci.* **2016**, *2*, 210–218.

(29) (a) Vermont, C. L.; van Dijken, H. H.; van Limpt, C. J.; de Groot, R.; van Alphen, L.; van Den Dobbelsteen, G. P. Antibody avidity and immunoglobulin G isotype distribution following immunization with a monovalent meningococcal B outer membrane vesicle vaccine. *Infect. Immun.* **2002**, *70* (2), 584–590. (b) Burton, D. R.; Gregory, L.; Jefferis, R. Aspects of the molecular structure of IgG subclasses. *Monogr. Allergy* **1986**, *19*, 7–35.

(30) (a) Zhang, Y.; Dominguez-Medina, C.; Cumley, N. J.; Heath, J. N.; Essex, S. J.; Bobat, S.; Schager, A.; Goodall, M.; Kracker, S.; Buckley, C. D.; et al. IgG1 Is Required for Optimal Protection after Immunization with the Purified Porin OmpD from *Salmonella* Typhimurium. *J. Immunol.* **2017**, *199*, 4103–4109. (b) Hazenbos, W. L. W.; Heijnen, I. A. F. M.; Meyer, D.; Hofhuis, F. M. A.; Renardel de Lavalette, C.; Schmidt, R. E.; Capel, P. J. A.; van de Winkel, J. G. J.; Gessner, J. E.; van den Berg, T. K.; et al. Murine IgG1 Complexes Trigger Immune Effector Functions Predominantly via FcγRIII (CD16)1. *J. Immunol.* **1998**, *161*, 3026–3032.

(31) Korsholm, K. S.; Petersen, R. V.; Agger, E. M.; Andersen, P. T-helper 1 and T-helper 2 adjuvants induce distinct differences in the magnitude, quality and kinetics of the early inflammatory response at the site of injection. *Immunology* **2010**, *129*, 75–86.

(32) Avci, F. Y.; Li, X.; Tsuji, M.; Kasper, D. L. A mechanism for glycoconjugate vaccine activation of the adaptive immune system and its implications for vaccine design. *Nat. Med.* **2011**, *17*, 1602–1609.

(33) Moor, K.; Fadlallah, J.; Toska, A.; Sterlin, D.; Balmer, M. L.; Macpherson, A. J.; Gorochov, G.; Larsen, M.; Slack, E. Analysis of bacterial-surface-specific antibodies in body fluids using bacterial flow cytometry. *Nat. Protoc.* **2016**, *11*, 1531–1553.

(34) (a) Kelly, D. F.; Pollard, A. J.; Moxon, E. R. Immunological memory: the role of B cells in long-term protection against invasive bacterial pathogens. *JAMA* **2005**, *294* (23), 3019–3023. (b) Pollard, A. J.; Perrett, K. P.; Beverley, P. C. Maintaining protection against invasive bacteria with protein-polysaccharide conjugate vaccines. *Nat. Rev. Immunol.* **2009**, *9*, 213–220.

(35) (a) Boero, E.; Vezzani, G.; Micoli, F.; Pizza, M.; Rossi, O. Functional assays to evaluate antibody-mediated responses against *Shigella*: a review. *Front. Cell. Infect. Microbiol.* **2023**, *13*, 1171213.

(b) Toh, Z. Q.; Higgins, R. A.; Mazarakis, N.; Abbott, E.; Nathanielsz, J.; Balloch, A.; Mulholland, K.; Licciardi, P. V. Evaluating Functional Immunity Following Encapsulated Bacterial Infection and Vaccination. *Vaccines (Basel)* **2021**, *9* (6), 677.

(36) Wang, C.-H.; Li, S.-T.; Lin, T.-L.; Cheng, Y.-Y.; Sun, T.-H.; Wang, J.-T.; Cheng, T.-J. R.; Mong, K. K. T.; Wong, C.-H.; Wu, C.-Y. Synthesis of *Neisseria meningitidis* Serogroup W135 Capsular Oligosaccharides for Immunogenicity Comparison and Vaccine Development. *Angew. Chem., Int. Ed.* **2013**, *52*, 9157–9161.

(37) Schneider, C.; Smith, D. F.; Cummings, R. D.; Boligan, K. F.; Hamilton, R. G.; Bochner, B. S.; Miescher, S.; Simon, H. U.; Pashov, A.; Vassilev, T.; et al. The human IgG anti-carbohydrate repertoire exhibits a universal architecture and contains specificity for microbial attachment sites. *Sci. Transl. Med.* **2015**, *7* (269), 269ra261.